Poly(styrene–ethylene oxide) Block Copolymer Micelle Formation in Water: A Fluorescence Probe Study[1]

Manfred Wilhelm,[2a] Cheng-Le Zhao,[2b] Yongcai Wang, Renliang Xu, and Mitchell A. Winnik*

Department of Chemistry and Erindale College, University of Toronto, Toronto, Ontario M5S 1A1, Canada

Jean-Luc Mura[2c] and Gérard Riess

Ecole National Superieure de Chimie, 33 rue Werner, 68093 Mulhouse Cedex, France

Melvin D. Croucher

Xerox Research Centre, 2660 Speakman Drive, Mississauga, Ontario L5K 2L1, Canada

Received May 4, 1990; Revised Manuscript Received August 3, 1990

ABSTRACT: Block copolymer micelle formation was studied by a combination of fluorescent probe and quasi-elastic light scattering (QELS) techniques. The polymers, polystyrene–poly(ethylene oxide) diblock and triblock copolymers, with $\bar{M}_n$ values ranging from 8500 to 29 000, form spherical micelles in water over the entire concentration range over which QELS signals can be detected. Pyrene (Py) in water (6×10^{-7} M) partitions between the aqueous and micellar phases, accompanied by three changes in the pyrene spectroscopy. There is a red shift in the excitation spectrum, a change in the vibrational fine structure of Py fluorescence (I_1/I_3 decreases from 1.9 to 1.2), and an increase in the fluorescence decay time (from 200 to ca. 350 ns) accompanying transfer of Py from an aqueous to a hydrophobic micellar environment. From these data, critical micelle concentrations (range: 1–5 mg/L) and partition coefficients (3×10^5) can be calculated.

Block copolymers of polystyrene (PS) and poly(ethylene oxide) (PEO) form spherical micelles in water when the length of soluble PEO is significantly longer than that of the insoluble PS portion of the molecule.[3,4] This behavior is common to both PS–PEO diblock and PEO–PS–PEO triblock copolymers. In analogy with low molecular weight surfactants, one defines the onset of intermolecular association as the critical micelle concentration (cmc), and the theories of polymer micellization[5] predict that in the presence of micelles, the concentration of free, unassociated block copolymers is close in magnitude to that of the cmc.

There are relatively few studies devoted to determination of cmc values for block copolymer micelles. Scattering techniques, which are very powerful for determining the size and shape of the micelles, are able to detect the onset of association only if the cmc occurs in a concentration region where these techniques are sensitive. For block copolymers in water, this is often not the case. For the examples considered here, the cmc values lie well below the smallest concentrations detectable by either Rayleigh or quasi-elastic light scattering (QELS).

Fluorescence techniques have been used with great success in the study of low molecular weight surfactant micelles.[6] They are useful not only for cmc determination but also for measuring the aggregation number of the micelles. By comparison, aqueous block copolymer systems have received scant attention.[7] Several years ago Ikema et al. reported very interesting results using 1-anilinonaphthalene fluorescence to probe micelle formation in a water-soluble block copolymer.[7a] Because the change in the fluorescence signal they observed occurred in a concentration region too small for a corresponding change to be observed by light scattering, the authors chose not to interpret this signal as an indication of the onset of polymer association. This absence of clear-cut results seems to have discouraged others from applying these methods. It is only recently that there has been an outburst of activity in the study of block copolymer micelles by fluorescence techniques.[8]

In a preliminary communication,[9] we reported how one could use a simple fluorescent probe method to detect the onset of association for PS–PEO and PEO–PS–PEO at concentrations on the order of 1 ppm (1 mg/L). In these experiments we examined the effect of polymer concentration on the fluorescence of pyrene present in water at near saturation, 6×10^{-7} M. Three features of the absorption and emission spectra change when micellization occurs. First, the low-energy band of the L_a ($S_2 \leftarrow S_0$) transition is shifted from 332.5 to 338 nm. Second, the lifetime of the pyrene fluorescence decay increases from 200 to ca. 350 ns, accompanied by a corresponding increase in the fluorescence quantum yield. Third, the vibrational fine structure changes, as the transfer of pyrene from a polar environment to a nonpolar one suppresses the allowedness of the symmetry-forbidden (0,0) band—the Ham effect.[10] This change is described in terms of the ratio I_1/I_3, the intensities, respectively, of the first and third bands in the pyrene fluorescence spectrum.[11]

This type of behavior is well-known by chemists in the area of low molecular weight surfactant micelles. The classic efforts by Thomas,[11a] Turro,[12] De Schryver,[13] Almgren,[14] Zana,[15] and others[6] were instrumental in promoting the explosive growth of knowledge about these systems. In the case of water-soluble polymers with hydrophobic components, the situation is more subtle. When the cmc is very low, the number of dye molecules present can equal or exceed the number of polymer molecules. One could easily imagine that partitioning of the fluorescent probe rather than polymer association would dominate the change in fluorescence signal. In the extreme example of polysoaps which form only single-molecule micelles, there is no multimolecular association and hence no cmc. Here one would observe only probe

0024-9297/91/2224-1033$02.50/0

Table I
Molecular Characteristics of Block Copolymers

sample	$\bar{M}_n$(PS)	$\bar{M}_n$(PEO)	$\bar{M}_n$(total)	$\bar{M}_w/\bar{M}_n$	PEO wt %
		Diblock Copolymers			
DB23	11 200	17 500	28 700	1.4	61
DB40	3 700	10 400	14 100	1.2	72
Jlm5	1 700	6 800	8 500	1.6	80
		Triblock Copolymers			
TB19	4 100	2 × 4500	13 100	1.4	68
TB51	1 800	2 × 9000	19 800	1.4	91
Jlm4	4 200	2 × 7900	20 000	1.1	79
Jlm6	3 600	2 × 7200	18 000	1.5	80
Jlm11	4 900	2 × 10500	25 900	1.2	81

partitioning between the hydrophobic and aqueous phases.[16]

Our approach in this paper is to examine in detail the fluorescence behavior of pyrene in water in the presence of poly(styrene–ethylene oxide) diblock and triblock copolymers in order to assess the factors that contribute to the signals we detect. We begin with the knowledge that these systems are in the form of micellar aggregates at all concentrations where they can be studied by light scattering.[17] From these experiments we know that diblock sample DB23 (see below) forms micelles of $\bar{M}_w = 8.3 \times 10^6$ with a number-averaged aggregation number $\bar{N}_n = 290$. Triblock sample TB19 forms micelles of $\bar{M}_w = 5.0 \times 10^5$ with $\bar{N}_n = 38$. These micelles are spherical and narrowly distributed in size. They have a core–shell type structure, which for DB23 has a (polystyrene) hard-core radius (r_c) of 11 nm and a hydrodynamic radius (R_H) of 22 nm. For TB19 the corresponding values are $r_c = 3.8$ nm and $R_H = 12$ nm. Although there is a slight tendency for the micelles to form loose aggregates at low concentrations, the size of the micelles themselves does not vary with block copolymer concentration for $c > 30$ mg/L.

Experimental Section

Polymer Synthesis. The polymer samples were synthesized in Mulhouse[18] using standard anionic polymerization techniques. Triblocks were initiated with potassium naphthalene; diblocks, with cumylpotassium. Aliquots of the "living" PS formed in the first stage at −78 °C in THF were quenched with degassed and slightly acidified methanol. These samples were analyzed by gel permeation chromatography (GPC) to determine $\bar{M}_n$ and $\bar{M}_w/\bar{M}_n$ of that block. After addition of purified ethylene oxide to the remaining "living" PS, the polymerization was carried out at room temperature for ca. 40 h. The copolymer was precipitated in heptane (DB and TB series) or in ether (Jlm series). The absence of PS and PEO homopolymers in the copolymer sample can be checked by GPC having dual detectors (UV and refractive index). The relative PS and PEO content of the copolymer was determined by ^{1}H NMR, elemental analysis, and UV spectroscopy. The molecular weight of the copolymer ($\bar{M}_n$(total)) is calculated from its composition and the molecular weight ($\bar{M}_n$) or the PS block. In the course of this work we discovered a problem with the initiation step of the diblock copolymers. Excessive vigor in the preparation of cumylpotassium led to incorporation of a polymer-bound fluorescent impurity absorbing light out to ca. 320 nm. An investigation of this problem is reported elsewhere.[19] The polymers and their characteristics are listed in Table I.

Sample Preparation. Stock solutions were prepared in two different ways: Initially these solutions were prepared by first dissolving the block copolymer (0.2–0.3 g) in tetrahydrofuran (THF) (ca. 5 mL) in a 100-mL volumetric flask. Water (Milli-Q, doubly distilled, 40 mL) was added with agitation, and then the flask was attached to a rotary evaporator to remove the THF (25 °C, water aspirator vacuum). This took 2–3 h, and foaming was sometimes a problem. When measured by gas chromatography, the aqueous solutions had residual THF concentrations of typically 150 ppm. This solution was then diluted with water to 100.0 mL.

A simpler method not involving cosolvents was developed. It was successful for all samples except DB23, in which the polystyrene content is too large. Here sufficient polymer was added to a volumetric flask to give a final concentration of 1.0 g/L. Doubly distilled (Milli-Q) water (40 mL) was added. The flask was heated at 60–70 °C for 1 h to dissolve the polymer and, after cooling, filled to the mark with additional water. This stock solution was diluted tenfold to yield a second solution which in turn was diluted two more times by a factor of ten to yield stock solutions varying in polymer concentration from 1.0 mg/L to 1.0 g/L.

To get sample solutions, a known amount of pyrene in acetone was added to each of a series of 10.0-mL volumetric flasks and the acetone evaporated. The amount was chosen to give a pyrene concentration in the final solution of either 6.0×10^{-7} M, similar to the saturation solubility of pyrene in water at 22 °C, or 1.2×10^{-7} M. To each flask was then added a measured amount of a stock solution, followed by doubly distilled water. The stoppered flasks were then heated for 3 h at 65 °C to equilibrate the pyrene and the micelles and subsequently allowed to cool overnight to room temperature. The samples ranged in polymer concentration from 2.0×10^{-4} to 1.0 g/L.

Fluorescence Measurements. For fluorescence measurements, ca. 2 mL of solution was placed in 11-mm cylindrical quartz or Pyrex tubes. In some instances 1.0 × 1.0 cm square cells were employed. All spectra were run on air-saturated solutions using a SPEX Fluorolog 2 spectrometer in the front-face geometry (22.5° collection optics) using slit openings of 0.5 mm. For fluorescence spectra, $\lambda_{ex} = 339$ nm, and for excitation spectra, $\lambda_{em} = 390$ nm. Spectra were accumulated with an integration time of 1 s/0.5 nm except for samples with [Py] = 1.2×10^{-7} M. Here signal-to-noise was improved significantly by using a 4 s/0.5 nm integration time.

Lifetimes were measured by the single-photon-timing technique.[20] Samples were excited with a pulsed-lamp source (0.5 atm D_2) using a home-built apparatus previously described.[21] In typical experiments (cf. Figure 7) we collected 20 000–40 000 counts in the initial channel. Decay profiles were fitted to a sum of exponential terms using the δ-function convolution method using POPOP (*p*-bis(5-phenyloxazol-2-yl)benzene) as a reference compound. No attempt was made to carry out a more sophisticated analysis of the decay profiles in terms of a distribution of pyrene lifetimes.[22] Pyrene in water always gave exponential $I(t)$ decays. Pyrene fluorescence also decayed exponentially (two decades, $\chi^2 \leq 1.3$; cf. Figure 7) at high polymer concentrations with lifetimes ranging from 320 to 360 ns. In some instances, mean decay times were calculated, $\langle \tau \rangle = \int tI(t)\,dt / \int I(t)\,dt$.

Hydrodynamic radii were determined by QELS initially at Guelph University and at SUNY, Stony Brook. These measurements have been described elsewhere.[17] Both nonnegative, nonlinear least squares (NNLS) and constrained regularized continuous inversion (CONTIN) algorithms were used in the ill-posed Laplace inversion of the intensity–intensity autocorrelation function from QELS to obtain the size distribution. Subsequent experiments were carried out in Toronto using a Brookhaven Model BI-90 particle sizer with a fixed 90° scattering angle. Comparable sets of information were obtained from all three instruments on samples where comparisons were made.

Results and Discussion

The polymers we examine were prepared by anionic polymerization. The structures, compositions, and molecular weights are presented in Table I. All the samples reported here have compositions rich in PEO. We attempted to extend these measurements to higher molecular weight diblock copolymers using samples given to us by Dr. T. Smith of the Xerox Webster Research Laboratory, Webster, NY. These samples contain 50 mol % or less PEO and fail to form stable solutions or suspensions in water.

Quasi-Elastic Light Scattering Measurements. The PEO-rich di- and triblock copolymers we examined all form spherical micelles in aqueous solution. Laplace inversion of the autocorrelation decay function obtained

Table II
Properties of PEO-PS Block Copolymer Micelles in Water

sample	x_{PS}[a]	I_1/I_3[b]	R_H,[c] nm	C_{app},[d] mg/L	cmc,[e] mg/L	$10^{-5}K_v$[f]
			Diblock Copolymers			
DB23	0.39	1.19	22	1.0	[g]	3
DB40	0.28	1.19	14	3.2	1.6 [1.0]	3.3
Jlm5	0.20	1.16	10	2.8	2.8 [2.9]	3.8
			Triblock Copolymers			
Tb19	0.32	1.19[h]	12	2.0	1.0 [2.5]	2.0
TB51	0.09		9	5.0		
Jlm4	0.21	1.20	13	2.8	2.7 [3.5]	
Jlm6	0.20	1.18	13	3.0	2.5 [3.7]	3.4
Jlm11	0.19	1.19	18	3.1	2.5 [3.0]	3.0

[a] Weight fraction of polystyrene. [b] Limiting value for pyrene fluorescence at large c. [c] Hydrodynamic radii from QELS. [d] Apparent cmc determined from excitation spectra; see text. [e] Determined by fitting $I_{338}/I_{332.5}$ data to eq 13 (values in brackets) and to eq 15. [f] From eq 13 except for sample DB23, which was determined from Figure 9. [g] Excitation spectra were not examined. [h] A smaller value was reported by us in ref 9. When these experiments were repeated, the value above was obtained.

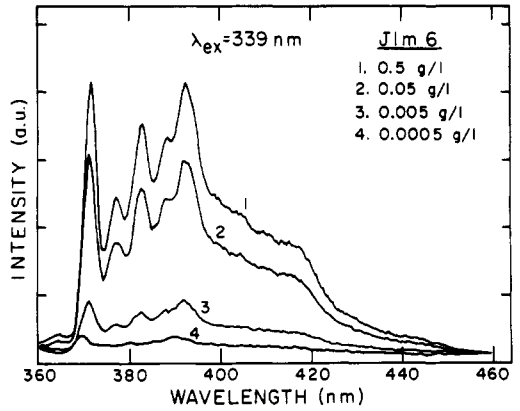

Figure 1. Fluorescence spectra of pyrene (6×10^{-7} M) in water in the presence of increasing concentrations of triblock copolymer sample Jlm6.

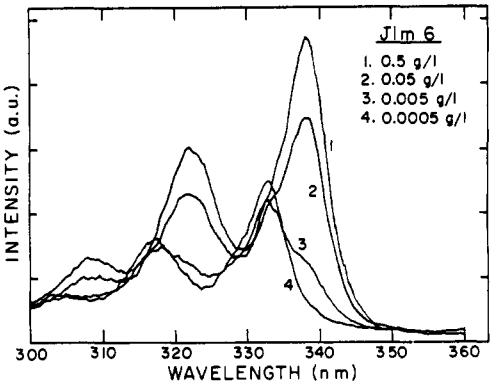

Figure 2. Excitation spectra, monitored at λ_{em} = 390 nm, for the same samples presented in Figure 1, showing the shift in the (0,0) band as pyrene partitions between aqueous and miceller environments.

from the QELS measurements indicates the presence of a bimodal size distribution, two very narrowly distributed species. The smaller more mobile species yielded hydrodynamic radii (R_H) consistent with the star model of block copolymer micelles[23] and correspond to individual micelles. We will examine this point in more detail in a forthcoming paper. The slower moving species contribute a signal whose relative intensity varies with block copolymer concentration and which disappears entirely at polymer concentrations above 100–200 mg/L.

In our previous report of the light scattering behavior of these block copolymers,[17] we attributed this signal to loose aggregates of micelles analogous to the secondary aggregates of micelles known to be formed from nonionic surfactants in water. In spite of its large contribution to the QELS signal, these aggregates represent only a small fraction of the block copolymer molecules present: reweighting the signal to account for the more intense scattering by the larger aggregates indicates that 99% or more of the block copolymer is present as simple micelles. In Table II we report R_H values only for the micelles themselves, and in the discussion that follows, we will ignore any possible consequences of secondary aggregation on the fluorescence behavior we observe.

Preliminary Fluorescence Probe Experiments. Fluorescence spectra of the Jlm6 triblock copolymer sample at various concentrations in the presence of 6×10^{-7} M pyrene are shown in Figure 1. The sample is excited at 339 nm. The spectrum is typical of pyrene fluorescence. The two noteworthy features of these spectra are that the intensity increases with increasing polymer concentration and that there are small changes in the intensity ratio of the first and third vibrational bands, I_1/I_3. The major

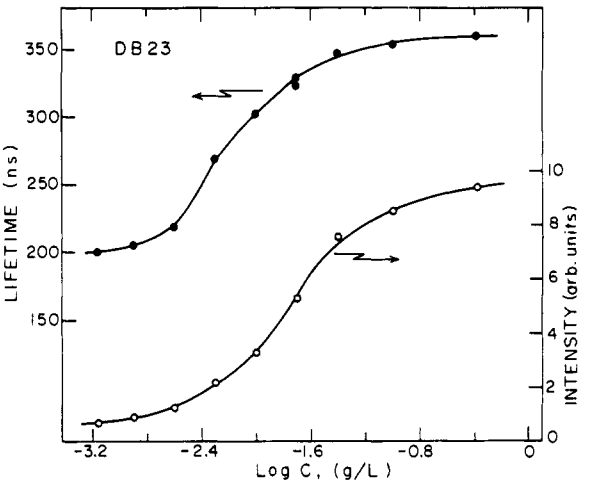

Figure 3. Plots of the mean decay time $\langle\tau\rangle$ (upper curve) and total fluorescence intensity (lower curve) for pyrene in water as a function of the concentration of diblock copolymer sample DB23.

contribution to the intensity change is the shift in the absorption and excitation spectra of the pyrene. As seen in Figure 2, pyrene in water has only a very small absorption at 339 nm, which increases substantially upon transfer to the less polar micellar domain. It is the increase in light absorbed that makes the largest contribution to the intensity increase seen in Figure 1. This point will be elaborated below.

In Figure 3 we plot the fluorescence intensity (I) and the mean fluorescence decay time $\langle\tau\rangle$ as a function of diblock copolymer concentration. Below a certain concentration ($c \approx 2.5$ mg/L) I is essentially constant, and

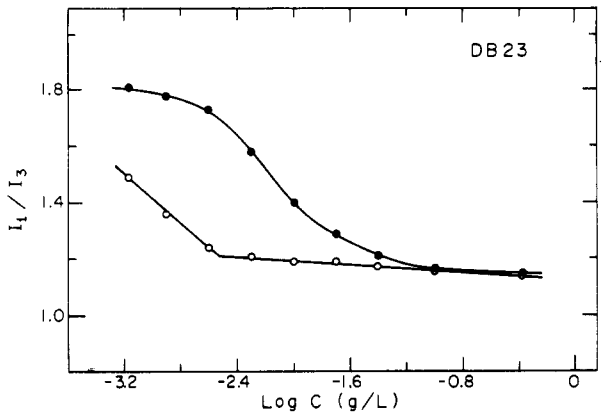

Figure 4. Plots of the ratio of intensities (I_1/I_3) of the vibrational bands in the pyrene fluorescence spectrum as a function of polymer concentration for the same samples shown in Figure 3. Top curve, λ_{ex} = 333 nm; bottom curve, λ_{ex} = 339 nm.

above this concentration, this intensity increases with increasing log c. This change in intensity reflects the onset of micelle formation and the partitioning of the pyrene between the aqueous and micellar phases. Over the same concentration range, $\langle\tau\rangle$ increases from 200 to 360 ns.

The I_1/I_3 peak height ratio (Figure 4) decreases over the concentration range of 0.2–2.5 mg/L and remains constant thereafter. The magnitude of I_1/I_3 in the high-concentration range (here 1.17) is somewhat higher than that for pyrene in a PS film (0.95) or in toluene solution (1.04) but significantly lower than that in water (1.9). The I_1/I_3 ratio for λ_{ex} = 339 or 340 nm is strongly weighted toward pyrenes in a hydrophobic environment. As one sees in Figure 4, changing the excitation wavelength to 333 nm weights this ratio in favor of the pyrene in an aqueous environment. The I_1/I_3 ratio is very helpful for determining the location of the pyrene probe in the micelles. Values of I_1/I_3 range from 1.15 to 1.20 and place the pyrene in the polystyrene core region of the micelle, influenced perhaps by the proximity of the polar surface. These values decrease slightly with increasing polymer concentration.

The plot in Figure 3 shows clear evidence for a change in signal in the region of 2 mg/L polymer. It is tempting to identify this value with the cmc. In this section we consider first two different ways of obtaining a value for the crossover point and then second, ambiguities in interpreting its meaning. Because of these ambiguities, we refer to these crossover concentrations as the apparent cmc (C_{app}) values.

One approach to the determination of C_{app} is to take the fluorescence intensities for λ_{ex} = 339 nm and fit the I vs log c plot to a sigmoidal curve. An example is shown in Figure 5. C_{app} (arrow in Figure 5) is taken as the intersection of the tangent to the curve at the inflection with the horizontal tangent through the points at low polymer concentration. Alternatively, we can examine the (0,0) bands in the pyrene excitation spectra and compare the intensity ratio $I_{338}/I_{332.5}$. At low concentrations this ratio takes the value characteristic of pyrene in water, and at high concentrations it takes the value of pyrene entirely in the hydrophobic environment. As one sees in Figure 6, a plot of $I_{338}/I_{332.5}$ vs log c is flat at the low-concentration extreme and sigmoidal in the crossover region. We define the value of the C_{app} in a similar way to that described above. This value is reproducible and has the advantage that the low-concentration values (0.30 ± 0.05) and the high-concentration values (2.1 ± 0.1) are essentially the same for all block copolymer samples. In

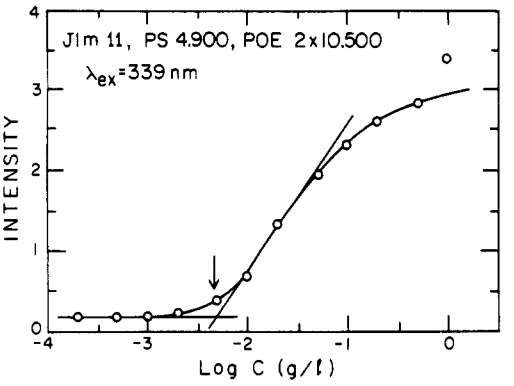

Figure 5. Plot of the fluorescence intensity of pyrene as a function of the concentration of triblock copolymer sample Jlm11, indicating how a value for C_{app} is obtained from the data.

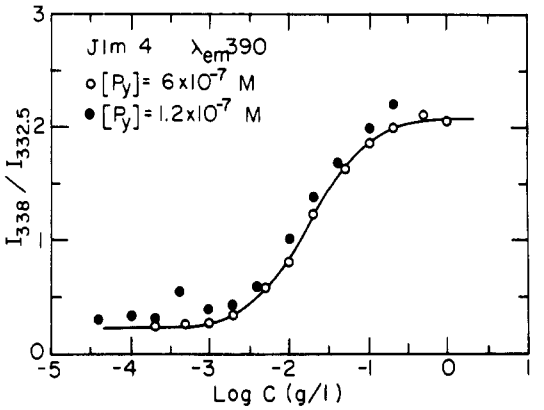

Figure 6. Plot of the intensity ratio $I_{338}/I_{332.5}$ (from pyrene excitation spectra) vs. log c for triblock copolymer sample Jlm4 for two different pyrene concentrations.

practice, the values for C_{app} from I vs log c and from $I_{338}/I_{332.5}$ vs log c are quite similar, with the former being somewhat more sensitive to scatter in the data. Values for the C_{app} values determined for the various samples are presented in Table II.

There is another much less interesting interpretation possible for the data in Figures 5 and 6. These sigmoidal curves have the shape one would anticipate for a binding isotherm plotted semilogarithmically. In such a case, the crossover in the low-concentration range would represent the point where the incremental increase in signal due to binding becomes smaller than the random error in determining the I value of the unbound component. Distinguishing this situation from a true onset of aggregation is a delicate problem. In this respect it is interesting to note that the C_{app} values obtained are all very similar, ranging from 1.0 to 5.0 mg/L, with six of the values clustering around 3 mg/L. The molar values cover a factor of 8 in concentration, and in the region of the apparent onset of association, the number of pyrene molecules in the sample exceeds the number of polymer molecules severalfold.

These are various approaches one can take to try to establish the influence on the data of a unimer–micelle equilibrium. One can determine whether C_{app} depends upon the pyrene concentration. If one had a larger spectrum of samples than we described here, one could examine whether C_{app} depends in some meaningful way upon polymer chain length. With sufficiently accurate data, one could assess whether the data fit better to a binding isotherm expressed in terms of (c = cmc) or in terms of the total polymer concentration c. Among the data reported here, only the $I_{338}/I_{332.5}$ intensity ratios

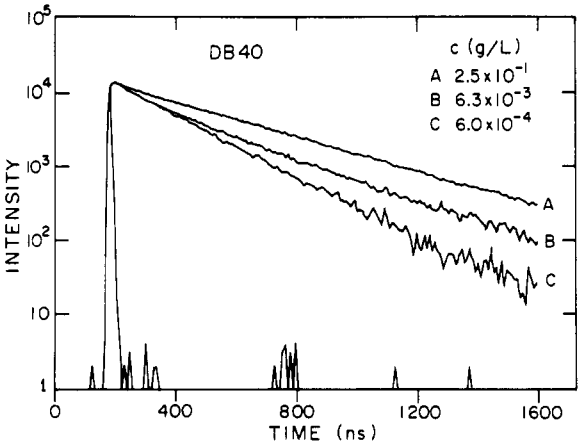

Figure 7. Fluorescence decay profiles for pyrene at 6.0×10^{-7} M in water in the presence of three different concentrations of diblock copolymer sample DB40.

obtained from the excitation spectra permit an unambiguous demonstration of the influence of the cmc on our experiments. This point will be considered as part of the following section, and we will conclude that C_{app}, determined as described above, is an upper bound to the cmc.

In order to test whether the phenomena reported here depend upon the pyrene concentration, we repeated certain experiments with a pyrene concentration of 1.2×10^{-7} M. As one sees in Figure 6, the lower pyrene concentration gives data that are similar to, but somewhat more scattered than, those for [Py] = 6.0×10^{-7} M. The data in Figure 6 show a small upward shift in the $I_{338}/I_{332.5}$ values for the low pyrene concentration data. Both sets of data, however, yield essentially identical values for C_{app}.

Pyrene Partitioning into the Micelles. The partitioning of pyrene into the micellar phase can, in principle, be determined from UV absorption spectra, excitation spectra, or fluorescence decay profiles [$I(t)$] for a set of samples spanning a range of polymer concentrations. In practice, both excitation spectra and the $I(t)$ measurements are able to provide the information needed.

Fluorescence Decay Profiles. Pyrene has a very different lifetime in water than in the micellar phase. In Figure 7 we show that, at high polymer concentration, pyrene decays exponentially with a lifetime (τ_m) of ca. 350 ns. There is some variation in this lifetime among different block copolymer samples. In water or at block copolymer concentrations below the cmc, the pyrene decay is also exponential, with a lifetime of 192 ns. At intermediate concentrations the decay is nonexponential, but when fit to a sum of two exponential terms, the decay times correspond to the values determined for pyrene in the aqueous and micellar phases. This type of phenomenon has been reported previously for surfactant micelles.[24] It suggests that $I(t)$ contains a superposition of two signals and that the prefactors of the exponential terms describe the fraction of pyrene in each phase.

$$I(t)/I(0) = A_m \exp(-t/\tau_m) + (1 - A_m) \exp(-t/\tau_w) \quad (1)$$

As a consequence, decay profiles were fit to eq 1 with τ_w fixed at 192 ns to obtain optimum parameters for A_m, the fraction of pyrene in the micellar phase. A plot of A_m vs log c for two samples is shown in Figure 8. This analysis presumes equal excitation of both populations of pyrenes and slow exchange of pyrenes between the two phases. The former requirement would be met by exciting the sample at a wavelength that is a near the isosbestic point for the absorbances of the water- and micelle-bound dyes. It is not well satisfied here, where λ_{ex} = 339 nm. The

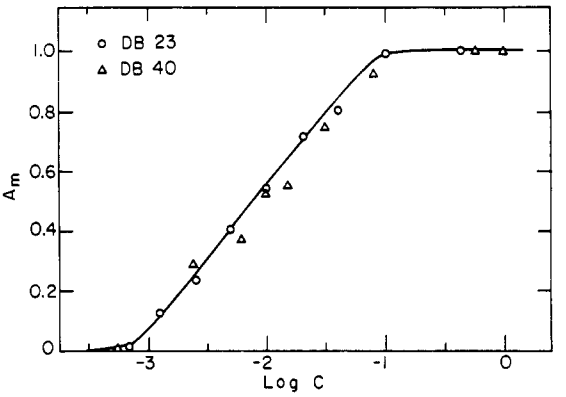

Figure 8. Plot of A_m, obtained by fitting pyrene fluorescence decay traces to eq 1, against log c for two different diblock copolymer samples. The line is simply drawn visually through the open-circle data points.

latter is established by the success in fitting the data to eq 1 over the entire range of polymer concentrations. As a consequence, we expect the A_m values shown in Figure 8 to be weighted in favor of the micelle-bound pyrenes. If there is a distribution of pyrene environments in the micelles, with a corresponding distribution of τ_m values, this adds an additional uncertainty in the interpretation of A_m, and by fitting our decay profiles to eq 1, we may well conceal an underlying distribution of τ_m values.[25]

Excitation Spectra. The intensity of fluorescence I due to sample excitation at wavelength λ can be written as

$$I = k\phi(1 - 10^{-\epsilon_\lambda l[Py]}) \quad (2)$$

with ϵ_λ, the molecular decadic extinction coefficient at wavelength λ, [Py] the molar pyrene concentration, l the cell path length, and k an instrumental constant. We can express the ratio of intensities in the excitation spectra $F = I_{338}/I_{332.5}$ as

$$F = \frac{\phi_w(1 - 10^{-\epsilon_{1w} l[Py]_w}) + \phi_m(1 - 10^{-\epsilon_{1m} l[Py]_m})}{\phi_w(1 - 10^{-\epsilon_{2w} l[Py]_w}) + \phi_m(1 - 10^{-\epsilon_{2m} l[Py]_m})} \quad (3)$$

where the subscripts j refer to the water (j = w) and micellar (j = m) phases, and for ϵ_{ij}, the molar decadic extinction coefficient

$$\epsilon_{ij}: \; i = 1 \text{ (338 nm)}, \text{ j = w (water)}$$

$$i = 2 \text{ (332.5 nm)}, \text{ j = m (micelle)}$$

Note that $[Py]_m$ refers to the concentration of micelle-bound pyrene averaged over the entire sample volume. Equation 3 could be evaluated if the appropriate ϵ_{ij} values in the two phases as well as the two quantum yields ϕ_j were known. Because ϕ_j is proportional to τ_j, we calculate that

$$\phi_m/\phi_w = \tau_m/\tau_w = 1.8 \quad (4)$$

An interesting feature of eq 3 can be appreciated by examining the spectra in Figure 2. While I_{338} (the numerator in eq 3) increases approximately sevenfold over the range of polymer concentrations, $I_{332.5}$ is essentially constant. If we set the denominator in eq 3 equal to a constant, we can write

$$F = \alpha[\phi_w(1 - 10^{-\epsilon_{1w} l[Py]_w}) + \phi_m(1 - 10^{-\epsilon_{1m} l[Py]_m})] \quad (5)$$

and note that at low concentration $F_{min} = 0.30 \pm 0.05$ and at high concentration $F_{max} = 2.1 \pm 0.1$. Expanding the Beer's law terms in (5) and considering a fixed pyrene concentration over the entire range of polymer concen-

trations, one finds that

$$\frac{F_{max}}{F_{min}} = \frac{\phi_m \epsilon_{1m}}{\phi_w \epsilon_{1w}} \tag{6}$$

or that $(\epsilon_{1m}/\epsilon_{1w}) = 3.9$. This value is in reasonable agreement with the values $\epsilon_{338}^{H_2O} = 17\,000\ M^{-1}\ cm^{-1}$ and $\epsilon_{1m} = 77\,000\ M^{-1}\ cm^{-1}$ measured independently.

In the intermediate range of polymer concentrations

$$\frac{F - F_{min}}{F_{max}} = \frac{[Py]_m}{[Py]}\left[1 - \frac{\epsilon_{1w}\phi_w}{\epsilon_{1m}\phi_m}\right] = \frac{[Py]_m}{[Py]}\left[1 - \frac{F_{min}}{F_{max}}\right] \tag{7}$$

or

$$\frac{[Py]_m}{[Py]} = \frac{F - F_{min}}{F_{max} - F_{min}} \tag{8}$$

and

$$\frac{[Py]_m}{[Py]_w} = \frac{F - F_{min}}{F_{max} - F} \tag{9}$$

which permits calculation of the fraction of pyrene ($[Py]_m/[Py]$) incorporated into the micelle or the ratio ($[Py]_m/[Py]_w$) of the pyrene in the two phases.

The Binding Equilibrium. Here we consider two aspects of the interaction of pyrene with the PS core of the micelle. First we consider the equilibrium constant K_v for partitioning of pyrene between the aqueous and micellar phases. Second we examine the evidence that our experiments are sensitive to the onset of block copolymer association (the true cmc). At modest polymer concentrations, $c > 30$ mg/L, we know from light scattering studies[17] that the micelles formed are large and spherical with PS core radii on the order of 6–12 nm. We presume therefore that pyrene binding to the micelles can be described as a simple partition equilibrium between a micellar (PS) phase of volume V_m and a water phase of volume V_w.

$$\frac{[Py]_m}{[Py]_w} = \frac{K_v V_m}{V_w} \tag{10}$$

$$\frac{[Py]}{[Py]_m} = 1 + \frac{V_w}{K_v V_m} \tag{11}$$

If the cmc for the block copolymer lies well below the C_{app} values determined above or if the fluorescence of pyrene is unaffected by cmc, we can write

$$\frac{[Py]_m}{[Py]_w} = \frac{K_v \chi_{PS} c}{1000 \rho_{PS}} \tag{12}$$

On the other hand, if the measurements are sensitive to micellar association of polymer molecules, eq 12 must be modified to take that effect into account.

$$\frac{[Py]_m}{[Py]_w} = \frac{K_v \chi_{PS}(c - cmc)}{1000 \rho_{PS}} \tag{13}$$

In the above expressions, χ_{PS} is the weight fraction of PS in the polymer and ρ_{PS} is the density of the PS core of the micelle, which we shall assume to take the same value (1.04 g/mL) as bulk polystyrene.

At large values of c ($c \gg C_{app}$), the two equations become indistinguishable but are nevertheless useful for determination of K_v. In Figure 9 we plot the results of our fluorescence decay data according to eq 11, setting $A_m = [Py]_m/[Py]$ and $V_m/V_w = \rho_{PS}\chi_{PS}c$. There is substantial scatter in the data, especially when A_m values are small. Values at log $c < -3.2$ have been deleted from the data in Figure 9. There is no indication of a cmc effect on pyrene partitioning, but we have too few data and too much scatter for experiments in the low polymer concentration region (ca. 10^{-3} g/L) to draw meaningful conclusions about this point. The data at larger c values are more reliable. The line fitted to the diblock copolymer samples in Figure 9 gives a value of $K_v = 3 \times 10^5$.

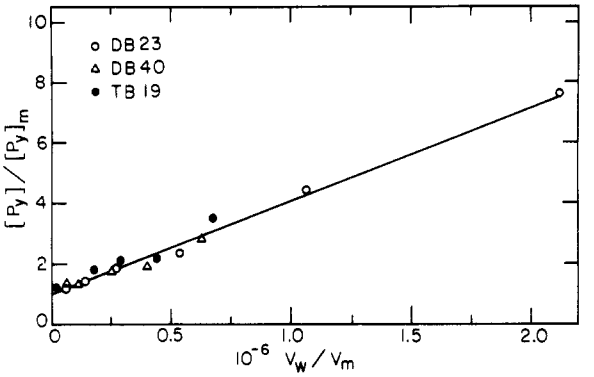

Figure 9. Plot of $[Py]/[Py]_m = A_m^{-1}$, obtained from fluorescence decay measurements, vs. V_w/V_m. See text and eq 11.

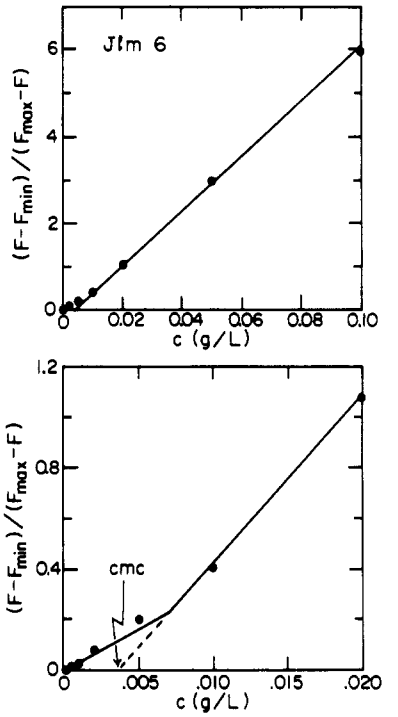

Figure 10. Plot of $(F - F_{min})/(F_{max} - F)$ vs. c for Jlm6 in water. The lower curve focuses on data in the low-concentration range.

The influence of the cmc is much more apparent in data taken from the excitation spectra. When these data are plotted according to eq 12, they can be fitted to two intersecting straight lines. An example is shown in Figure 10 for sample Jlm6. At high concentration (upper plot), the slope of the line is $(K_v\chi_{PS}/1000\rho_{PS})$, from which K_v can be calculated. Below the cmc, one would expect $(F - F_{min})$ to be zero if there were no tendency of pyrene to bind to the isolated block copolymer chains. The fact that these values increase with c at low concentrations suggests that there is a small contribution to the pyrene signal due to pyrene association with isolated polymer chains or to premicellar aggregates. If this is the case, then the cmc can be identified as the extrapolated intercept with the c axis of the line with slope $(K_v\chi_{PS}/10^3\rho_{PS})$.

Confirmation of this idea is possible by inverting eq 12 and 13 and replotting the data as a function of inverse

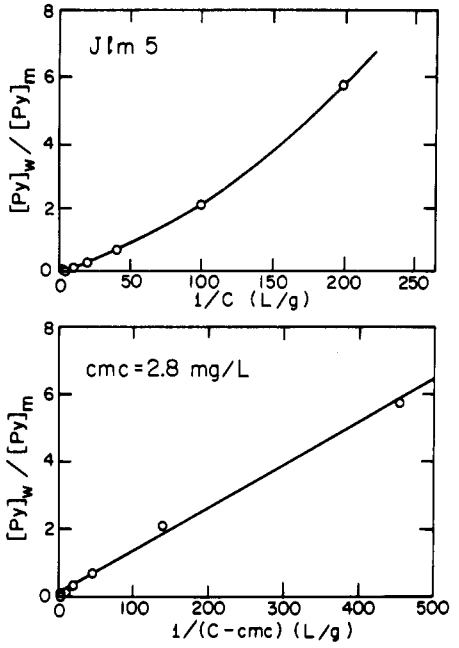

Figure 11. Plots of $[Py]_w/[Py]_m$ vs. c^{-1} (upper graph) and vs. $(c - cmc)^{-1}$ (lower graph) for diblock copolymer sample Jlm5. The value chosen for the cmc is 2.8 mg/L.

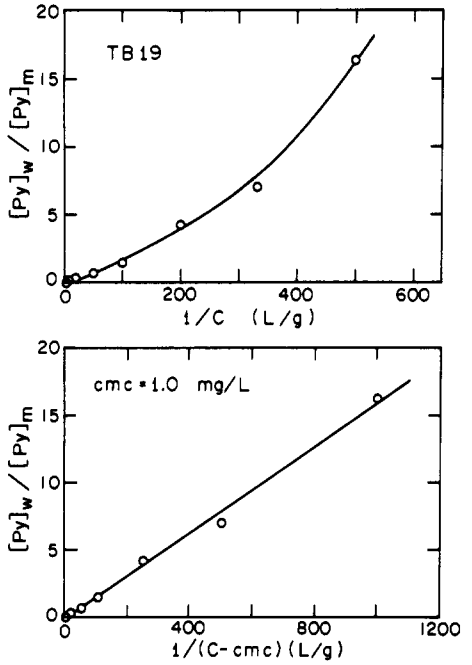

Figure 12. Plots of $[Py]_w/[Py]_m$ vs. c^{-1} (upper graph) and vs. $(c - cmc)^{-1}$ (lower graph) for triblock copolymer sample TB19. The value chosen for the cmc is 1.0 mg/L.

polymer concentration:

$$\frac{F_{max} - F}{F - F_{min}} = \frac{1000\rho_{PS}}{K_v \chi_{PS} c} \tag{14}$$

or

$$\frac{F_{max} - F}{F - F_{min}} = \frac{1000\rho_{PS}}{K_v \chi_{PS}(c - cmc)} \tag{15}$$

In Figures 11 and 12 we examine the information available from the excitation spectra as a function of c^{-1}. Results for diblock copolymer sample Jlm5 are shown in Figure 11, and results for triblock sample TB19, are shown in Figure 12. The upper graphs present plots against total inverse polymer concentration, i.e., eq 14. There is a clear indication of upward curvature for both plots, and this type of behavior is seen for every one of our block copolymer samples. When the data are replotted according to eq 15 (lower graphs), the data give much better linear fits. These results provide compelling evidence that the concentration dependence of the excitation spectra is sensitive to cmc.

Careful examination of the data provides several important insights into the experiment. First, we find that plots according to eq 15 sometimes fail to give linear traces when $[Py]_w/[Py]_m$ is plotted against $(c - C_{app})$. Excellent straight lines can be obtained by choosing a cmc value smaller than C_{app} but well within the experimental uncertainty in the original C_{app} determination. This is a useful result because it indicates that fitting the data either to eq 12 or to eq 15 with cmc as a variable parameter is a much more sensitive way to determine cmc accurately. It is also evident that when the data are plotted in this way, fitted values of both cmc and K_v are very sensitive to experiments performed in the range of c = 1.2–5 times cmc. In future experiments it will be important to focus our data collection in this concentration regime to determine accurate cmc values. Such experiments will be particularly important in the case where one has sufficient samples within a systematic series, i.e., M_{PS} constant with variable M_{PEO}, so that the factors that influence the magnitude of cmc can be clearly established.

Values of cmc and K_v determined from these experiments are reported in Table II. In almost every case, cmc is smaller than C_{app}, which suggests that C_{app} determined by the recipe described above provides only an estimated upper bound to cmc. K_v values are all on the order of 3×10^5 (dimensionless). A number of this magnitude indicates that partitioning of pyrene into the PS phase is strongly favored and that the large amount of pyrene in the aqueous phase is a consequence of the tiny volume fraction of PS in the samples.

Our K_v value can be compared to the molar value K_{eq} (M^{-1}) obtained by Almgren et al.[26] for partitioning of pyrene into sodium dodecyl sulfate (SDS) micelles. These authors determined a value of $K_{eq} = 17 \times 10^5 M^{-1}$, where M is the molar micelle concentration. SDS micelles have an aggregation number of 62, and assuming the molar volume of the $C_{12}H_{25}$ chains to be that of dodecane, we calculate $K_v = 1.2 \times 10^5$ for their system. This value is about half the value we report here and suggests that pyrene partitioning into the PS core of these block copolymer micelles is favored by about a factor of 2 over its partitioning into SDS micelles.

Conclusions

Polystyrene–poly(ethylene oxide) diblock and triblock copolymers form spherical micelles in water solution with a dense core composed of the insoluble PS component. When traces of pyrene are added to these solutions, the pyrene partitions into the core phase. Several aspects of its spectroscopic properties are changed upon transfer into the more hydrophobic environment. The (0,0) band is shifted from 332 nm (H_2O) to 338 nm. The vibrational fine structure (the I_1/I_3 ratio) undergoes the changes expected for this kind of transfer, and the fluorescence lifetime increases from 200 ns (H_2O) to ca. 350 ns in the micelle. By examining the extent of these changes as a function of block copolymer concentration, one can identify and determine the critical micelle concentration, here on the order of 1–3 mg/L, and determine as well the partition coefficient K_v for pyrene. For the various samples we examined, K_v values ranged from 2×10^5 to 4×10^5.

Acknowledgment. We thank NSERC Canada and the Province of Ontario through its URIF program for their support of this research. M.W. thanks the Deutsche Akademische Austausch Dienst for supporting his stay in Toronto.

References and Notes

(1) Paper no. 3 in a series on polymer micelle formation. For paper no. 2, see ref 17.
(2) Current addresses: (a) Department of Chemistry, Johannes Gutenberg University, Mainz, West Germany; (b) BASF Canada, Sarnia, ON, Canada; (c) NUROLOR, Verneuil-en-Halatte, France.
(3) For reviews of block copolymers and their colloidal properties, see: (a) Tuzar, Z.; Kratochvil, P. *Adv. Colloid Interface Sci.* **1976**, *6*, 201. (b) Price, C. In *Developments in Block Copolymers*; Goodman, I., Ed.; Applied Science Publishers: London, 1982; Vol. 1, pp 39–80. (c) Riess, G.; Hurtrez, G.; Bahadur, P. *Encyclopedia of Polymer Science and Engineering*, 2nd ed.; Wiley: New York, 1985; Vol. 2, pp 324–434. (d) Tuzar, Z.; Kratochvil, P. *Colloids Surf.*, in press.
(4) (a) Riess, G.; Rogez, D. *Polym. Prepr. (Am. Chem. Soc., Div. Polym. Chem.)* **1982**, *23*, 19. (b) Rogez, D. Doctoral Thesis, University of Haute Alsace, Mulhouse, France, 1987.
(5) (a) Leibler, L.; Orland, H.; Wheeler, J. C. *J. Chem. Phys.* **1983**, *79*, 3550. (b) Noolandi, J.; Hong, K. M. *Macromolecules* **1982**, *15*, 482; **1983**, *16*, 1443. (c) Whitmore, M. D.; Noolandi, J. *Macromolecules* **1985**, *18*, 657. (d) Munch, M. R.; Gast, A. P. *Macromolecules* **1988**, *21*, 1360.
(6) For reviews, see: (a) Kalyanasundaram, K. *Photochemistry in Microheterogenous Systems*; Academic Press: Orlando, FL, 1987. (b) Turro, N. J.; Grätzel, M.; Braun, A. *Angew. Chem., Int. Ed. Engl.* **1980**, *19*, 675 and references cited therein.
(7) (a) Ikema, M.; Odagiri, N.; Tanaka, S.; Shinohara, I.; Chiba, A. *Macromolecules* **1981**, *14*, 34; **1982**, *15*, 281. (b) Turro, N. J.; Cheung, C. J. *Macromolecules* **1984**, *17*, 2123.
(8) (a) Tang, W. T.; Hadziioannou, G.; Smith, B. A.; Frank, C. *Polymer* **1988**, *29*, 1313. (b) Major, M. D.; Torkelson, J. M.; Brearly, A. M. *Macromolecules* **1990**, *23*, 1700, 1711.
(9) Zhao, C. L.; Winnik, M. A.; Riess, G.; Croucher, M. D. *Langmuir* **1990**, *6*, 514.
(10) Ham, J. S. *J. Chem. Phys.* **1953**, *21*, 756.
(11) (a) Kalyanasundaram, K.; Thomas, J. K. *J. Am. Chem. Soc.* **1977**, *99*, 2039. (b) Dong, D. C.; Winnik, M. A. *Can. J. Chem.* **1984**, *62*, 2560.
(12) Turro, N. J.; Yekta, A. *J. Am. Chem. Soc.* **1975**, *97*, 2488; **1974**, *96*, 306.
(13) Dederen, J. C.; vander Auweraer, M.; De Schryver, F. C. *Chem. Phys. Lett.* **1979**, *68*, 451.
(14) Almgren, M.; Löfroth, J. E. *J. Colloid Interface Sci.* **1981**, *81*, 486.
(15) (a) Lianos, P.; Zana, R. *Chem. Phys. Lett.* **1980**, *76*, 62. (b) Lianos, P.; Zana, R. *J. Colloid Interface Sci.*, **1981**, *84*, 100.
(16) Chu, D.-Y.; Thomas, J. K. *Macromolecules* **1987**, *20*, 2133.
(17) Xu, R.; Winnik, M. A.; Hallett, R.; Riess, G.; Croucher, M. D. *Macromolecules* **1991**, *24*, 87.
(18) (a) Finaz, G.; Rempp, P.; Parrod, J. *Bull. Soc. Chim. Fr.* **1962**, 262. (b) For details, see: Mura, J. L. Doctoral thesis, University of Haute Alsace, Mulhouse, France (submitted, 1990) and ref 4b.
(19) Hruska, Z.; Winnik, M. A.; Hurtrez, G.; Riess, G. *Polym. Commun.* **1990**, *31*, 402.
(20) (a) O'Connor, D. V.; Phillips, D. *Time-Correlated Single Photon Counting*; Academic Press: London, 1984. (b) Zuker, M.; Szabo, A. G.; Bramall, L.; Kvajcarski, D. T.; Selinger, B. *Rev. Sci. Instrum.* **1985**, *56*, 14.
(21) Martinho, J. M. G.; Egan, L. S.; Winnik, M. A. *Anal. Chem.* **1987**, *59*, 861.
(22) (a) Siemiarczuk, A.; Ware, W. R. *J. Phys. Chem.* **1989**, *93*, 7609. (b) Livesey, A. K.; Brochon, J. C. *Biophys. J.* **1987**, *52*, 693.
(23) Halperin, A. *Macromolecules* **1987**, *20*, 2943.
(24) (a) Van Bockstaele, M.; Gelan, J.; Martens, H.; Put, J.; Dederen, J. C.; Boens, N.; De Schryver, F. C. *Chem. Phys. Lett.* **1978**, *58*, 211. (b) Hautala, R. R.; Schore, N. E.; Turro, N. J. *J. Am. Chem. Soc.* **1973**, *95*, 5508.
(25) James, D. R.; Ware, W. R. *Chem. Phys. Lett.* **1986**, *126*, 7.
(26) Almgren, M.; Grieser, F.; Thomas, J. K. *J. Am. Chem. Soc.* **1979**, *101*, 279.

Registry No. (PS)(PEO) (block copolymer), 107311-90-0; pyrene, 129-00-0.